HHS Public Access

Author manuscript

Curr Biol. Author manuscript; available in PMC 2016 March 02.

Published in final edited form as:

Curr Biol. 2015 March 2; 25(5): 546–555. doi:10.1016/j.cub.2014.12.049.

Rph1/KDM4 mediates nutrient-limitation signaling that leads to the transcriptional induction of autophagy

Amélie Bernard[1], **Meiyan Jin**[1], **Patricia González-Rodríguez**[2], **Jens Füllgrabe**[2], **Elizabeth Delorme-Axford**[1], **Steven K. Backues**[1,3], **Bertrand Joseph**[2], and **Daniel J. Klionsky**[1,*]

[1]Life Sciences Institute, and the Department of Molecular, Cellular and Developmental Biology, University of Michigan, Ann Arbor, MI 48109, USA

[2]Department of Oncology Pathology, Cancer Centrum Karolinska, Karolinska Institutet, Stockholm 17176, Sweden

Summary

Background—Autophagy is a conserved process mediating vacuolar degradation and recycling. Autophagy is highly upregulated upon various stresses and is essential for cell survival in deleterious conditions. Autophagy defects are associated with severe pathologies, whereas unchecked autophagy activity causes cell death. Therefore, to support proper cellular homeostasis, the induction and amplitude of autophagy activity have to be finely regulated. Transcriptional control is a critical, yet largely unexplored, aspect of autophagy regulation. In particular little is known about the signaling pathways modulating the expression of autophagy-related genes, and only a few transcriptional regulators have been identified as contributing in the control of this process.

Results—We identified Rph1 as a negative regulator of the transcription of several *ATG* genes and a repressor of autophagy induction. Rph1 is a histone demethylase protein, but it regulates autophagy independently of its demethylase activity. Rim15 mediates the phosphorylation of Rph1 upon nitrogen starvation, which causes an inhibition of its function. Preventing Rph1 phosphorylation or overexpressing the protein causes a severe block in autophagy induction. A similar function of Rph1/KDM4 is seen in mammalian cells, indicating that this process is highly conserved.

Conclusion—Rph1 maintains autophagy at a low level in nutrient-rich conditions; upon nutrient limitation, the inhibition of its activity is a prerequisite to the induction of *ATG* gene transcription and autophagy.

*Correspondence: klionsky@umich.edu; Tel 734-615-6556; Fax 734-647-9702.

[3]Present address: Department of Chemistry, Eastern Michigan University, Ypsilanti, MI 48197, USA

Supplemental Information

Supplemental Information includes Supplemental Experimental Procedures, four figures and five tables and can be found with this article online at XXXX.

Keywords

autophagy; lysosome; vacuole; stress; yeast

Introduction

Macroautophagy (hereafter referred to as autophagy) is a highly conserved pathway during which portions of the cytoplasm, superfluous or damaged organelles, or invasive pathogens are delivered to the vacuole (in yeast and plants) or the lysosome (in mammals) for degradation and subsequent recycling. Morphologically, autophagy starts with the nucleation of the phagophore, the initial membrane structure, at a peri-vacuolar site called the phagophore assembly site, or PAS (Figure S1A, [1]). Through the acquisition of lipids, the phagophore then expands, surrounding its cargo, and ultimately seals to generate a double-membrane vesicle called the autophagosome. After autophagosome fusion with the vacuole, the inner membrane of the vesicle as well as its cargo are degraded and recycled into the cytosol. The macromolecules resulting from this pathway are then used by the cell to maintain cellular homeostasis during deleterious conditions [2].

Autophagy is highly upregulated upon multiple stress conditions and notably nutrient limitation where it plays critical roles in cell adaptation and survival [3]. The autophagy pathway plays a role in cellular physiology, and mammalian development as well as the immune response [4–6], and autophagy impairments are associated with various human pathologies such as cancer or metabolic diseases [7–8]. Autophagy also occurs at a constitutive basal level in physiological conditions. In yeast, the cytoplasm-to-vacuole targeting (Cvt) pathway is essential for the biosynthetic delivery of vacuolar enzymes during growth [9]. In mammals, basal autophagy functions in the quality control machinery involved in the degradation of damaged organelles and protein aggregates which, when accumulated, lead to various neurodegenerative disorders such as Huntington, Alzheimer and Parkinson diseases [10].

If a sub-optimal autophagy activity can be detrimental, a supra-optimal level can also be deleterious for the cells; uncontrolled autophagy leads to cell death [11–12], certain microbes rely on autophagy to provide nutrients [13], and cancer cells can also use autophagy to help survive in an unfavorable environment [14]. Therefore, to support proper cellular functions, rates of autophagy have to be finely regulated. Over the past 20 years, extensive molecular studies of autophagy have led to the identification of the core components of the autophagy machinery, encoded by the autophagy-related (*ATG*) genes (for review see ref. [15]); yet the regulatory pathways governing their functions remain largely unknown. In particular the transcriptional regulation of the *ATG* genes is still mostly unexplored (for review see ref. [14]).

The expression of most of the *ATG* genes, and their corresponding proteins, highly increases upon autophagy induction after nitrogen starvation [16]. Given the energy cost for such an induction, it has been suggested that this upregulation is critical for the normal modulation of autophagy and for the pathway to reach full amplitude when most needed. Furthermore, the reported abnormal expression of several *ATG* genes in various human diseases supports

the proposed physiological importance of their transcriptional regulation [17–20]. Recent studies in yeast identified Ume6 as a transcriptional repressor of *ATG8* [21] and showed that the level of Atg8 controls the size of the autophagosome [22]. Conversely, the level of Atg9, regulated by Pho23, controls the frequency of formation (hence the number) of autophagosomes [16]. Nevertheless, very few transcription factors have been identified as regulating the expression of *ATG* genes in either yeast or mammals and the contribution of the induction of specific *ATG* genes in autophagy activity is still poorly understood.

At the starting point of this study a search for new transcriptional regulators of autophagy was initiated by the screen of a collection of over 150 mutants lacking a single transcription factor or DNA-binding protein. Analysis of the expression of a set of *ATG* genes in this library led to the identification of Rph1 as a master transcriptional repressor of autophagy.

Results

Rph1 Is a Transcriptional Repressor of *ATG* Genes

In order to identify transcriptional regulators of autophagy we compared the expression of a subset of *ATG* genes in wild-type cells to that in a library of DNA binding protein deletion mutants. *ATG1*, *ATG7*, *ATG8*, *ATG9*, *ATG14* and *ATG29* were selected as target genes because they encode proteins involved in different steps of the autophagy pathway (Figure S1A) and because they show a strong induction after nitrogen starvation, indicating that they are under transcriptional control in these conditions (Figure 1A,B; [16]). The DNA binding protein mutants displayed a range of phenotypes (data not shown), and *rph1*Δ in particular showed a significant upregulation of *ATG7*, *ATG8*, *ATG9*, *ATG14* and *ATG29* accompanied with a modest induction of *ATG1* in growing conditions (Figure 1A, Table S1, Table S2). Similarly, the deletion of *RPH1* resulted in an increased expression of *ATG32* (Figure 1A), a marker of mitophagy (the selective autophagic degradation of mitochondria). In contrast, deleting *RPH1* had essentially no effect on the transcription of *ATG10*, an autophagy-related gene that displays no change in expression in response to nitrogen deprivation (Figure 1A,B). Additionally, there was no significant difference in the mRNA levels of *ATG* genes between the *rph1*Δ strain and wild-type cells after starvation (Figure 1B). This difference between growing and starvation conditions suggests that Rph1 represses the expression of nitrogen-sensitive *ATG* genes specifically in nutrient-replete conditions.

Rph1 is a DNA-binding protein, which contains two C_2H_2 zinc-finger motifs as well as a Jumonji C histone demethylase catalytic domain. Rph1 has a paralog, Gis1, and previous studies report that Rph1 and Gis1 have distinct as well as overlapping targets [23–26]. Whereas the deletion of *GIS1* had a very minor effect on the expression of some of the *ATG* genes that we examined, the *gis1*Δ *rph1*Δ double mutant showed an enhanced induction of the mRNA level of these genes compared to the single *RPH1* deletion in growing conditions (Figure 1A,B). This finding indicates that Rph1 plays a predominant role in the regulation of *ATG* genes, but that its absence can be partially compensated by Gis1.

Consistent with the changes observed at the mRNA levels, *rph1*Δ cells showed a strong enrichment of the proteins Atg7, Atg8, Atg9, Atg14 and Atg29 and a modest increase in Atg1 compared to the wild type; in contrast the level of Atg10 was unaffected (Figure 1C–E,

Figure S1B,C). This phenotype was exacerbated in *gis1*Δ *rph1*Δ cells as suggested by the analysis of Atg7 and Atg8 (Figure 1C,D). It is worth noting that although the abundance of Atg1, Atg8, Atg9 and Atg14 was higher in *rph1*Δ cells in rich conditions compared to the wild type (Figure 1C, compare lanes 3 and 5, Figure S1B,C), the protein levels were still lower than those seen after starvation (Figure 1C, compare lanes 5 and 6, Figure S1B,C), indicating that other pathways are contributing to the regulation of the corresponding genes. In contrast, deleting *RPH1* alone was sufficient to increase the Atg7 protein abundance to a higher level than that seen after 3 h of nitrogen starvation in the wild-type cells (Figure 1D, compare lanes 6 and 7, Figure S1B,C), suggesting that Rph1 has a preponderant role in regulating the expression of Atg7. Together these results show that Rph1 is a transcriptional repressor of *ATG* genes.

Rph1 Is a Negative Regulator of Autophagy

Finding that Rph1 represses the expression of *ATG* genes in growing conditions suggests that it might be a negative regulator of autophagy. To test this hypothesis autophagy activity was measured using a Pho8Δ60 assay in which alkaline phosphatase activity reflects autophagy amplitude [27]. After 1 h of nitrogen starvation, the wild-type cells displayed a substantial induction of alkaline phosphatase activity (50% of the activity seen at 3 h; note that the wild-type activity is set to 100% at each time point in Figure 2A), which was blocked by the deletion of *ATG7* (Figure 2A). Compared to the wild type, autophagy was induced to a higher level in the *rph1*Δ cells and *gis1*Δ *rph1*Δ cells; in contrast the deletion of *GIS1* alone had no significant effect. We extended this analysis by using a GFP-Atg8 processing assay [28]. After one hour of starvation, autophagy was induced more rapidly and to a higher extent in the *rph1*Δ and *gis1*Δ *rph1*Δ cells, as indicated by the level of free GFP compared to the wild-type (Figure 2B,C). Note that the enhanced autophagy activity in *rph1*Δ cells upon short-term nitrogen starvation was attenuated after a prolonged time of induction. This observation is consistent with the fact that deleting *RPH1* increases the transcription of *ATG* genes only in nutrient-rich conditions; a higher abundance of Atg proteins can therefore support a jump-start in autophagy activity upon its induction by nitrogen starvation. After prolonged starvation, Atg protein levels in wild-type cells reach that of the mutant strains, abolishing the difference in autophagy activity relative to the *rph1*Δ and *gis1*Δ *rph1*Δ mutants.

Our results indicated that Rph1 has a major role in the transcriptional regulation of *ATG7* (Figure 1, Figure S1B,C). Atg7 is an E1 activating enzyme, which notably mediates the conjugation of Atg8 to PE and is critical for autophagy (Figure 2A). Nevertheless, very little is known concerning the effect of *ATG7* transcriptional regulation on autophagy. To address this, an *atg7*Δ strain was transformed with plasmids in which protein A (PA)-tagged Atg7 was placed under the control of promoters (*FLO5*, *GAL3*, *ATG7* and *SEF1* in increasing order of strength) with different transcriptional activities (Figure 3A). Note that in these conditions we did not observe a strong increase in the abundance of Atg7-PA in wild-type cells after starvation (compared to Figure 1D and Figure S1B,C), which may reflect expression from a plasmid as opposed to the complete *ATG7* promoter. Lowering Atg7 abundance correlated with a reduction of Atg8–PE conjugates (Figure 3A) as well as a reduction in autophagy activity (Figure 3B). The finding that Atg7 protein amount directly

affects autophagy activity supports a model in which Rph1 regulates autophagy in part by controlling the expression of Atg7. Nevertheless, an increase in Atg7 protein alone was not sufficient to induce autophagy (Figure 3B, +N) suggesting that the *rph1*Δ phenotype results from the combined upregulation of multiple *ATG* genes.

The overexpression of Rph1 inhibits autophagy and decreases cell survival in nitrogen starvation conditions

To further test the role of Rph1 in autophagy, *RPH1* was overexpressed under the control of the *ZEO1* promoter (Figure 4A). Overexpression of Rph1 caused a severe block in the induction of several *ATG* genes after starvation (Figure 4B) but had no effect on the expression of *ATG1*. Furthermore, the reduction in *ATG* transcripts correlated with a decrease in autophagy activity (Figure 4C). A decrease in autophagy flux could either result from a reduction in the number of autophagosomes or a reduction in their size. To distinguish between the two hypotheses, cells overexpressing Rph1 were further analyzed using transmission electron microscopy (TEM). After 2 h of nitrogen starvation, cells overexpressing Rph1 displayed a strong reduction in the average number of autophagic bodies accumulated in the vacuole compared to wild-type cells (Figure 4D,E, Figure S2, Table S3); in contrast there was no significant effect on the size of the autophagic bodies (Figure 4D,F, Figure S2, Table S3).

Next, the physiological importance of the Rph1-dependent regulation of autophagy was tested by monitoring the survival phenotype of cells overexpressing Rph1 after nitrogen starvation. Wild-type yeast cells showed no significant cell death during the time course of the experiment, whereas a complete block of autophagy in *atg1*Δ cells resulted in a complete loss of viability (Figure 4G). In comparison, cells overexpressing Rph1 exhibited a slight growth defect in nitrogen-replete conditions (Figure 4G, left panel) and showed a reduced survival rate after prolonged starvation (Figure 4G, right panel). Together these results suggest that overexpressed-Rph1 promotes cell death by repressing autophagosome biogenesis and thereby inhibiting autophagy.

Rph1 DNA Binding Ability but Not Histone Demethylase Activity Is Required for its Function in Autophagy

Rph1 is a Jumonji C (JmjC)-containing histone demethylase protein, which is the only demethylase targeting H3K36 tri-methylation in *Saccharomyces cerevisiae* [29]. Previous studies showed that the transcriptional repression of some Rph1 targets is dependent on its histone demethylase activity [30]. We therefore proposed that Rph1 may repress *ATG* genes transcription, and thereby autophagy, in a similar manner. This idea was first tested using a *set2*Δ deletion strain; Set2 is the histone methyltransferase mediating H3K36 methylation in yeast cells [31] and, in this regard, has an opposite function to that of Rph1. Nitrogen starvation did not significantly affect H3K36 tri-methylation (H3K36me3) and *rph1*Δ cells did not show any difference in the H3K36me3 status compared to wild-type cells (Figure 5A). In contrast, the deletion of *SET2* led to a complete block in H3K36me3 marks. Nevertheless, we did not observe an autophagy defect in *set2*Δ cells compared to the wild type (Figure 5B), which indicates that the level of H3K36me3 does not regulate autophagy.

Next, we analyzed the previously described Rph1^{H235A} mutant in which the replacement of histidine 235 with alanine inhibits the protein's histone demethylase activity (Figure S3A,B; [30]). Protein analysis verified the stability of Rph1^{H235A} compared to wild-type Rph1 (Figure 5C). The *rph1*Δ phenotype was restored to the same extent by either wild-type Rph1 or Rph1^{H235A} (Figure 5D, Figure S3C). In addition, cells overexpressing Rph1 or the Rph1^{H235A} mutant showed a similar reduction in autophagy activity compared to wild-type cells (Figure 5E,F). Together these results show that the function of Rph1 in autophagy is, at least mostly, independent of its histone demethylase activity.

Previous results from a large-scale ChIP-chip (chromatin immunoprecipitation-on-chip) analysis identified several *ATG* genes as potential direct targets of Rph1 [32]. Consistent with this idea, a DNA motifs search in the promoter region of *ATG* genes identified one or multiple Rph1-binding consensus sites in 23 out of 32 *ATG* genes (Table S4, Table S5). In particular, our analysis revealed the presence of the environmentally regulated Rph1 binding site (TWAGGG; [26]) in the promoter of highly regulated genes such as *ATG7*, *ATG9* and *ATG14* and of a related site (AGGGG) in *ATG8* and *ATG29* but not in those of a modestly affected gene, *ATG1*, or a non-affected gene, *ATG10*. Therefore we tested the importance of the DNA-binding domain of the protein by constructing an Rph1$^{\Delta Z}$ mutant, in which the deletion of both zinc-finger motifs at the C-terminal part of the protein prevents DNA binding ([31]; Figure S3A). A ChIP approach showed a 2-fold enrichment of Rph1-PA at the *ATG7* promoter compared to Rph1$^{\Delta Z}$-PA (Figure 5G). A similar enrichment was found at the *PHR1* promoter, which was used as a positive control [30], but not at the non-coding region located at the tip of chromosome VI (ChrVI-260K), which was used as a negative control. This indicates that Rph1 directly binds the promoter region of *ATG7* and that this binding is significantly reduced upon deletion of the zing-finger domains of the protein. Furthermore, even though Rph1$^{\Delta Z}$-PA was found over-accumulated compared to Rph1-PA (Figure 5C), this mutant form of the protein was unable to rescue the *ATG* gene overexpression phenotype or the increased autophagy activity induction of the *rph1*Δ cells (Figure 5D, Figure S3C), thus showing that the DNA-binding domain of Rph1 is strictly required for its function in autophagy. Together these results show that the histone demethylase activity of Rph1 is not required for its function in autophagy and suggest that, instead, Rph1 represses the expression of *ATG* genes by restricting the access of the transcriptional machinery or potential activators at these loci as has been proposed for other Rph1-regulated genes [23, 33].

Rph1 Phosphorylation upon Nitrogen Starvation Releases its Repression of Autophagy

As mentioned above, the deletion of *RPH1* induced the expression of *ATG* genes in rich conditions but had no effect on mRNA levels after nitrogen starvation (Figure 1). These results suggest a model in which Rph1 represses the transcription of these targets when cells grow in nutrient-replete medium and that upon nitrogen starvation this repression is released thereby allowing the induction of *ATG* genes and autophagy. Previous studies describe Rph1 as a phosphoprotein and show that Rph1 phosphorylation inhibits its activity [23]. Similarly, we observed a shift in the molecular weight of Rph1-PA as well as the appearance of a faint upper band in conditions of nitrogen depletion, suggesting that Rph1 undergoes phosphorylation at multiple sites (Figure 6A, left panel, and Figure 6C). This shift was

accompanied by a modest decrease in protein level shortly after nitrogen starvation (Figure 6A,C). In order to get a better resolution of the phosphorylation status of Rph1 we used Phos-tag, a molecule that binds specifically to phosphorylated ions, thereby increasing the molecular weight of phospho-isoforms. With addition of Phos-tag, Rph1-PA was observed as several higher molecular weight bands in nitrogen starvation conditions compared to rich conditions, strongly supporting the hypothesis that Rph1 is phosphorylated upon starvation (Figure 6A, right panel). Note that this analysis also revealed Rph1-PA as a doublet in rich conditions (Figure 6A, right panel) indicating that the protein undergoes some phosphorylation even in the presence of nitrogen. Furthermore, phosphatase treatment of the protein samples prevented the changes in Rph1 mobility demonstrating that the change in migration represents genuine phosphorylation of the protein (Figure 6B).

To test the importance of Rph1 phosphorylation for autophagy induction, we next aimed to identify the phosphorylated residues upon nitrogen starvation. In order to identify such sites we used previously published data from large-scale phosphoproteomic analyses. In particular Huber et al. [34] identified 5 sites (group II, Figure S4) at which phosphorylation was suggested to be upregulated upon treatment with rapamycin, a drug that induces autophagy; in addition the work by Bodenmiller et al. [35], proposed that phosphorylation at T411 and S412 (group I, Figure S4) is upregulated when the gene encoding Tpk2, a subunit of the autophagy repressor PKA, is deleted. Based on these data we generated Rph1 mutants where the phosphoresidues in group I or group I and II were mutated to alanine. In addition serine 429 which is also predicted to be phosphorylated was mutated to alanine because of its proximity to the residues in group I. The mutants showed only a partial reduction in phosphorylation based on gel migration, and a concomitant accumulation of the non-phosphorylated form of the protein after starvation (Figure S4B). Accordingly, autophagy activity was only reduced to a minor, yet significant, level in these mutants (Figure S4C), suggesting that additional residues that were not identified by mass spectrometry may also be involved in phospho-regulation of Rph1. Together these results show that residues in group I and II participate in the phosphorylation of Rph1 after starvation and suggest that this modification of the protein inhibits its activity upon autophagy induction.

Rim15 Mediates the Phosphorylation of Rph1 upon Nitrogen Starvation thereby inducing Autophagy

Next, we attempted to identify the kinase responsible for Rph1 phosphorylation prior to autophagy activation; Rim15 appeared to be a good candidate as it is phosphorylated and translocated into the nucleus after nitrogen starvation at which time it activates autophagy [36–38]. Analysis of Rph1-PA showed a strong block in Rph1 molecular mass shift when *RIM15* was deleted (Figure 6C,D) showing that this kinase is, at least partly, responsible for Rph1 phosphorylation upon nitrogen starvation. Moreover, the inhibition of Rph1 phosphorylation in the *rim15*Δ cells was accompanied by a stabilization of the Rph1 protein compared to wild-type cells where the protein level decreased after nitrogen starvation. In addition, the *RIM15* deletion caused a partial block in the induction of some of the *ATG* genes and Atg proteins that we analyzed, concomitant with the reduction of autophagy activity seen in the same conditions (Figure 6E,F and Figure S4D–F). Furthermore, deletion of *RPH1* in the *rim15*Δ cells rescued the defect in Atg7-PA level in response to nitrogen

starvation (Figure 6G), showing that Rim15 acts upstream of Rph1 to regulate *ATG7* expression during autophagy.

These findings strongly support the idea that the Rim15-dependent phosphorylation of Rph1 is required for proper induction of autophagy upon nitrogen starvation. Our previous work showed that Rim15 also phosphorylates Ume6 leading to an inhibition of Ume6 activity and an upregulation of *ATG8* after nitrogen starvation [21]. As previously described, the *ume6*Δ cells showed an increase in the expression of *ATG8* in nutrient-rich conditions compared to the wild type ([21], Figure S4G); this was accompanied by an upregulation of *ATG1* and *ATG9*. In contrast the expression of *ATG7*, *ATG14* and *ATG29* was unaffected by the deletion of *UME6*. Because *rph1*Δ cells showed higher expression of *ATG7* and *ATG29* we suggest that the block of, at least, *ATG7* and *ATG29* induction in the *rim15*Δ cells is specifically due to the loss of Rph1 phosphorylation and propose that this contributes to the reduction of autophagy activity in this mutant background.

The Regulation of Autophagy by Rph1/KDM4 Is Conserved from Yeast to Mammals

To test if the mechanism of autophagy regulation that we uncovered here was conserved in higher eukaryotes we studied the role of one mammalian homolog of *RPH1*, *KDM4A*, in the autophagy pathway. A reduction of KDM4A level was associated with an increase in the mRNA level of several *ATG* genes including *ATG7*, *WIPI1* and *ATG14*, whereas there was essentially no effect on *MAP1LC3B* (Figure 7A). HeLa cells transformed with si*KDM4A* showed an accumulation of LC3-II compared to control cells pointing to an increase in basal autophagy in this condition (Figure 7B, left panel). To verify that the increase in LC3-II reflected an upregulation of autophagy rather than a block in flux, we treated the cells with the autophagy inhibitor bafilomycin A_1. We detected a further increase in the level of LC3-II upon the addition of bafilomycin A_1, suggesting that the knockdown of KDM4A did not interfere with, but instead enhanced, autophagic flux. Conversely, the overexpression of KDM4A led to a reduction in the level of LC3-II compared to control cells (Figure 7B, right panel) further supporting the conclusion that KDM4A is a repressor of autophagy.

To extend this analysis, we monitored the autophagic flux using a tandem reporter construct, mRFP-GFP-LC3, a probe that allows distinction between autophagosomes (AP, GFP^+ RFP^+, yellow puncta, Figure 7C) and autolysosomes (AL, GFP^- RFP^+, red puncta, Figure 7C). Compared to the control, cells knocked down for KDM4A showed an increase in yellow puncta representing autophagosomes, in both basal autophagy (DMSO) conditions or after autophagy induction by Torin1 (Figure 7C,D). Following Torin1 treatment there was an increase in autolysosomes in both the control and si*KDM4A* cells, again indicating that autophagic flux was not inhibited by KDM4A depletion.

We found that the level of KDM4A was reduced in response to Torin1 treatment (Figure 7E) indicating that KDM4A is degraded in this condition. A previous phosphoproteomic analysis indicated that KDM4A is phosphorylated at residue Y547 [39]; analysis of KDM4A with a phosphospecific antibody directed towards Y547 showed that phosphorylation at this residue is upregulated by treatment with Torin1. Together, these results suggest that, similar to Rph1, the phosphorylation of KDM4A acts as a switch to promote autophagy induction in mammalian cells.

Discussion

In this study, a screen for transcription factors modulating *ATG* gene expression identified Rph1 as a transcriptional repressor of autophagy. We show that Rph1 is a negative regulator of the expression of, at least, *ATG7*, *ATG8*, *ATG9*, *ATG14* and *ATG29*. Consistent with our results, a recent microarray analysis reported the induction of *ATG7*, and *ATG14*, as well as *ATG16*, *ATG17*, *ATG23* and *ATG24* in *rph1*Δ cells in physiological conditions [23] suggesting that Rph1 might control a large set of *ATG* genes.

Our results show that the deletion of *RPH1* can be partially complemented by Gis1, its paralog, indicating that Gis1 plays a minor role in the regulation of *ATG* genes. Rph1 and Gis1 are JmjC-domain containing proteins; while Rph1 histone demethylase activity is well established [29], controversies exist concerning Gis1 [29, 40]. Whether or not Gis1 is catalytically active, its JmjC domain is not required for its transcriptional activity [24,41]. Similarly we show here that the histone demethylase activity of Rph1 is not required for its control of autophagy, but that its DNA binding domain is critical. Rph1 and Gis1 share a high homology in their C_2H_2 zinc finger DNA-binding domain suggesting that they could bind similar motifs, which might explain the partial redundancy between the two proteins. Yet, the deletion of *RPH1* has a strong effect on the expression of *ATG* genes and affects autophagy activity, whereas deleting *GIS1* alone did not affect autophagy suggesting that Rph1 has higher affinity for the promoters of *ATG* genes and plays a major role in the repression of autophagy in nitrogen-replete conditions.

The deletion of *RPH1* has no effect on the expression of *ATG* genes after nitrogen depletion, and the phenotype of the *RPH1* null strain is attenuated after prolonged starvation suggesting that the activity of the protein is repressed in this condition. Indeed, we found that Rph1 is phosphorylated in a Rim15-dependent manner upon nitrogen starvation and that this phosphorylation is accompanied with a partial degradation of the protein. Inhibition of Rph1 phosphorylation or overexpression of the protein leads to a strong block of *ATG* gene induction as well as autophagy activity, showing that the phosphorylation of Rph1 represses its activity and is a prerequisite for autophagy induction. Altogether, these data propose a model in which, by repressing the expression of *ATG* genes, Rph1 maintains autophagy at a low level in nutrient-replete conditions. Upon nitrogen starvation, Rim15 mediates Rph1 phosphorylation, which causes a partial autophagy-independent degradation of the protein and an inhibition of its activity (Figure 6, Figure S4 and data not shown). This leads to a release of Rph1 repression of *ATG* genes, an induction of their expression and an overall induction of autophagy activity.

Rim15 controls many aspects of the nutrient-regulatory pathways, including autophagy, by integrating signals from TORC1 and PKA [38, 42]; yet little is known about the downstream effectors in these signaling pathway. We show that Rim15 phosphorylates Rph1, thereby releasing its repression of the expression of several *ATG* genes including *ATG7* and *ATG29*, upon nutrient limitation. Conversely, although Rph1 controls the expression of *ATG14*, its expression was not affected by the deletion of *RIM15*. Rim15 is under the control of both positive and negative regulators of autophagy [38], and it is therefore possible that the result of competitive effectors controlling the expression of *ATG14* account for this observation.

Uncovering the Rim15-dependent Rph1-mediated transcriptional control of autophagy here brings further comprehension to the overall signaling pathways leading to autophagy induction upon starvation.

How does the level of *ATG* gene transcription regulate autophagy activity? Several *ATG* genes show higher expression after nitrogen starvation ([16]; Figure 1), suggesting that this increase is required to support optimal autophagy activity; yet the physiological relevance of the induction of particular *ATG* genes is still largely unknown. Our previous work showed that the amount of Atg9 correlates with the number of autophagosomes [16], whereas the induction of *ATG8* promotes the formation of larger autophagosomes [22] thereby leading to an increase in the amount of cargo delivered to the autophagy pathway. Here we show that Rph1 plays a major role in the control of the expression of *ATG7*. Upon autophagy induction, Atg7 functions in the formation of Atg8–PE conjugates, which is a prerequisite to the membrane recruitment of Atg8 and the elongation of the phagophore [45]. Our results show that negatively modulating the expression of *ATG7* causes defects in autophagy activity (Figure 3), suggesting that the amount of Atg7 is rate limiting in the lipidation of the large pool of newly synthesized Atg8 after starvation. It is therefore tempting to speculate that, upon autophagy induction, a concomitant upregulation of both *ATG7* and *ATG8* is strictly required to support efficient autophagosome formation and thereby an increase in the magnitude of autophagy activity.

Besides its role in cell survival upon starvation, autophagy activity is also critical for cellular clearance of protein aggregates and damaged organelles, which, when accumulated, result in severe pathologies, such as neurodegenerative diseases [10]. Interestingly, a recent genomic study of sporadic Parkinson disease patients identified mutations in the *ATG7* promoter causing decreased ATG7 expression [17]. In this context, our finding that the transcriptional control of *ATG7* is critical for autophagy activity points to the physiological importance of the Rph1-mediated control of autophagy that we identified here. In particular, we show that the function of Rph1 is conserved from yeast to mammals. Four isoforms of KDM4, the homolog of Rph1, are present in mammalian cells. Here we show that KDM4A is a negative regulator of autophagy; whether other isoforms are also involved in this process remains to be investigated. Knocking down KDM4A increased autophagy activity, especially at base line, suggesting that modulating this novel regulatory pathway could be a good target for the development of disease therapies.

Experimental Procedures

Yeast Strains, Media and Culture

Gene disruptions were performed using a standard method [44]. Yeast cells were grown in YPD or SMD [16] and autophagy was induced in SD-N [16]. The yeast strains used in this study are listed in Table S1.

HeLa cells were purchased from Sigma and grown in MEM supplemented with penicillin/streptomycin, L-glutamine, non-essential amino acids and sodium pyruvate.

RNA and RT-qPCR

RNA was extracted using the RNeasy mini kit (Qiagen), and RNA was reverse-transcribed using the High-capacity cDNA Reverse Transcription kit (Applied Biosystems). See the supplement for details.

Chromatin Immunoprecipitation

ChIP was performed as previously described [45] with minor modifications as described in the supplement.

Transmission electron microscopy

TEM and sample analysis were performed as previously described [16].

Mammalian Cell Transfection

HeLa cells were transfected with siRNA using Lipofectamine 2000 reagent (Invitrogen) as described in the supplement.

Supplementary Material

Refer to Web version on PubMed Central for supplementary material.

Acknowledgments

This work was supported by NIH grant GM053396 to DJK, and by grants from the Swedish Cancer Society, the Swedish Childhood Cancer Foundation and the Swedish Research Council to BJ.

Abbreviations

Atg	autophagy-related
GFP	green fluorescent protein
PA	protein A
TEM	transmission electron microscopy

References

1. Lenstra TL, Benschop JJ, Kim T, Schulze JM, Brabers NA, Margaritis T, van de Pasch LA, van Heesch SA, Brok MO, Groot Koerkamp MJ, et al. The specificity and topology of chromatin interaction pathways in yeast. Mol Cell. 2011; 42:536–549. [PubMed: 21596317]
2. Xie Z, Klionsky DJ. Autophagosome formation: core machinery and adaptations. Nat Cell Biol. 2007; 9:1102–1109. [PubMed: 17909521]
3. Tsukada M, Ohsumi Y. Isolation and characterization of autophagy-defective mutants of *Saccharomyces cerevisiae*. FEBS Lett. 1993; 333:169–174. [PubMed: 8224160]
4. Levine B, Klionsky DJ. Development by self-digestion: molecular mechanisms and biological functions of autophagy. Dev Cell. 2004; 6:463–477. [PubMed: 15068787]
5. Deretic V, Levine B. Autophagy, immunity, and microbial adaptations. Cell Host Microbe. 2009; 5:527–549. [PubMed: 19527881]
6. Shi CS, Shenderov K, Huang NN, Kabat J, Abu-Asab M, Fitzgerald KA, Sher A, Kehrl JH. Activation of autophagy by inflammatory signals limits IL-1beta production by targeting

ubiquitinated inflammasomes for destruction. Nat Immunol. 2012; 13:255–263. [PubMed: 22286270]

7. Huang J, Klionsky DJ. Autophagy and human disease. Cell Cycle. 2007; 6:1837–1849. [PubMed: 17671424]
8. Mizushima N, Levine B, Cuervo AM, Klionsky DJ. Autophagy fights disease through cellular self-digestion. Nature. 2008; 451:1069–1075. [PubMed: 18305538]
9. Lynch-Day MA, Klionsky DJ. The Cvt pathway as a model for selective autophagy. FEBS Lett. 2010; 584:1359–1366. [PubMed: 20146925]
10. Nixon RA. The role of autophagy in neurodegenerative disease. Nat Med. 2013; 19:983–997. [PubMed: 23921753]
11. Chen Y, Azad MB, Gibson SB. Superoxide is the major reactive oxygen species regulating autophagy. Cell Death Differ. 2009; 16:1040–1052. [PubMed: 19407826]
12. Levine B, Yuan J. Autophagy in cell death: an innocent convict? J Clin Invest. 2005; 115:2679–2688. [PubMed: 16200202]
13. Ravikumar B, Sarkar S, Davies JE, Futter M, Garcia-Arencibia M, Green-Thompson ZW, Jimenez-Sanchez M, Korolchuk VI, Lichtenberg M, Luo S, Massey DC, Menzies FM, Moreau K, Narayanan U, Renna M, Siddiqi FH, Underwood BR, Winslow AR, Rubinsztein DC. Regulation of mammalian autophagy in physiology and pathophysiology. Physiol Rev. 2010; 90:1383–1435. [PubMed: 20959619]
14. Jin M, Klionsky DJ. Regulation of autophagy: Modulation of the size and number of autophagosomes. FEBS Lett. 2014; 588:2457–2463. [PubMed: 24928445]
15. Parzych KR, Klionsky DJ. An overview of autophagy: morphology, mechanism, and regulation. Antioxid Redox Signal. 2014; 20:460–473. [PubMed: 23725295]
16. Jin M, He D, Backues SK, Freeberg MA, Liu X, Kim JK, Klionsky DJ. Transcriptional regulation by pho23 modulates the frequency of autophagosome formation. Curr Biol. 2014; 24:1314–1322. [PubMed: 24881874]
17. Chen D, Pang S, Feng X, Huang W, Hawley RG, Yan B. Genetic analysis of the ATG7 gene promoter in sporadic Parkinson's disease. Neurosci Lett. 2013; 534:193–198. [PubMed: 23295909]
18. Liu H, He Z, von Rutte T, Yousefi S, Hunger RE, Simon HU. Down-regulation of autophagy-related protein 5 (ATG5) contributes to the pathogenesis of early-stage cutaneous melanoma. Sci Transl Med. 2013; 5:202ra123.
19. Wang J, Pan XL, Ding LJ, Liu DY, Da-Peng L, Jin T. Aberrant expression of Beclin-1 and LC3 correlates with poor prognosis of human hypopharyngeal squamous cell carcinoma. PLoS ONE. 2013; 8:e69038. [PubMed: 23935917]
20. Jo YK, Kim SC, Park IJ, Park SJ, Jin DH, Hong SW, Cho DH, Kim JC. Increased expression of ATG10 in colorectal cancer is associated with lymphovascular invasion and lymph node metastasis. PLoS ONE. 2012; 7:e52705. [PubMed: 23285162]
21. Bartholomew CR, Suzuki T, Du Z, Backues SK, Jin M, Lynch-Day MA, Umekawa M, Kamath A, Zhao M, Xie Z, et al. Ume6 transcription factor is part of a signaling cascade that regulates autophagy. Proc Natl Acad Sci U S A. 2012; 109:11206–11210. [PubMed: 22733735]
22. Xie Z, Nair U, Klionsky DJ. Atg8 controls phagophore expansion during autophagosome formation. Mol Biol Cell. 2008; 19:3290–3298. [PubMed: 18508918]
23. Liang CY, Wang LC, Lo WS. Dissociation of the H3K36 demethylase Rph1 from chromatin mediates derepression of environmental stress-response genes under genotoxic stress in Saccharomyces cerevisiae. Mol Biol Cell. 2013; 24:3251–62. [PubMed: 23985319]
24. Jang YK, Wang L, Sancar GB. RPH1 and GIS1 are damage-responsive repressors of PHR1. Mol Cell Biol. 1999; 19:7630–7638. [PubMed: 10523651]
25. Zhang N, Oliver SG. The transcription activity of Gis1 is negatively modulated by proteasome-mediated limited proteolysis. J Biol Chem. 2010; 285:6465–6476. [PubMed: 20022953]
26. Orzechowski Westholm J, Tronnersjo S, Nordberg N, Olsson I, Komorowski J, Ronne H. Gis1 and Rph1 regulate glycerol and acetate metabolism in glucose depleted yeast cells. PLoS One. 2012; 7:e31577. [PubMed: 22363679]

27. Noda T, Klionsky DJ. The quantitative Pho8Delta60 assay of nonspecific autophagy. Methods Enzymol. 2008; 451:33–42. [PubMed: 19185711]
28. Shintani T, Klionsky DJ. Cargo proteins facilitate the formation of transport vesicles in the cytoplasm to vacuole targeting pathway. J Biol Chem. 2004; 279:29889–29894. [PubMed: 15138258]
29. Tu S, Bulloch EM, Yang L, Ren C, Huang WC, Hsu PH, Chen CH, Liao CL, Yu HM, Lo WS, et al. Identification of histone demethylases in Saccharomyces cerevisiae. J Biol Chem. 2007; 282:14262–14271. [PubMed: 17369256]
30. Liang CY, Hsu PH, Chou DF, Pan CY, Wang LC, Huang WC, Tsai MD, Lo WS. The histone H3K36 demethylase Rph1/KDM4 regulates the expression of the photoreactivation gene PHR1. Nucleic Acids Res. 2011; 39:4151–4165. [PubMed: 21296759]
31. Strahl BD, Grant PA, Briggs SD, Sun ZW, Bone JR, Caldwell JA, Mollah S, Cook RG, Shabanowitz J, Hunt DF, et al. Set2 is a nucleosomal histone H3-selective methyltransferase that mediates transcriptional repression. Mol Cell Biol. 2002; 22:1298–1306. [PubMed: 11839797]
32. Venters BJ, Wachi S, Mavrich TN, Andersen BE, Jena P, Sinnamon AJ, Jain P, Rolleri NS, Jiang C, Hemeryck-Walsh C, et al. A comprehensive genomic binding map of gene and chromatin regulatory proteins in Saccharomyces. Mol Cell. 2011; 41:480–492. [PubMed: 21329885]
33. Nordberg N, Olsson I, Carlsson M, Hu GZ, Orzechowski Westholm J, Ronne H. The histone demethylase activity of Rph1 is not essential for its role in the transcriptional response to nutrient signaling. PLoS one. 2014; 9:e95078. [PubMed: 24999627]
34. Huber A, Bodenmiller B, Uotila A, Stahl M, Wanka S, Gerrits B, Aebersold R, Loewith R. Characterization of the rapamycin-sensitive phosphoproteome reveals that Sch9 is a central coordinator of protein synthesis. Genes Dev. 2009; 23:1929–1943. [PubMed: 19684113]
35. Bodenmiller B, Wanka S, Kraft C, Urban J, Campbell D, Pedrioli PG, Gerrits B, Picotti P, Lam H, Vitek O, Brusniak MY, Roschitzki B, Zhang C, Shokat KM, Schlapbach R, Colman-Lerner A, Nolan GP, Nesvizhskii AI, Peter M, Loewith R, von Mering C, Aebersold R. Phosphoproteomic analysis reveals interconnected system-wide responses to perturbations of kinases and phosphatases in yeast. Sci Signal. 2010; 3:rs4. [PubMed: 21177495]
36. Pedruzzi I, Dubouloz F, Cameroni E, Wanke V, Roosen J, Winderickx J, De Virgilio C. TOR and PKA signaling pathways converge on the protein kinase Rim15 to control entry into G0. Mol Cell. 2003; 12:1607–1613. [PubMed: 14690612]
37. Wanke V, Pedruzzi I, Cameroni E, Dubouloz F, De Virgilio C. Regulation of G0 entry by the Pho80–Pho85 cyclin–CDK complex. EMBO J. 2005; 24:4271–4278. [PubMed: 16308562]
38. Yang Z, Geng J, Yen WL, Wang K, Klionsky DJ. Positive or negative roles of different cyclin-dependent kinase Pho85-cyclin complexes orchestrate induction of autophagy in Saccharomyces cerevisiae. Mol Cell. 2010; 23:250–264. [PubMed: 20417603]
39. Tao WA, Wollscheid B, O'Brien R, Li XJ, Bodenmiller B, Watts JD, Hood L, Aebersold R. Quantitative phosphoproteome analysis using a dendrimer conjugation chemistry and tandem mass spectrometry. Nat Methods. 2005; 2:591–598. [PubMed: 16094384]
40. Klose RJ, Kallin EM, Zhang Y. JmjC-domain-containing proteins and histone demethylation. Nat Rev Genet. 2006; 7:715–727. [PubMed: 16983801]
41. Yu Y, Neiman AM, Sternglanz R. The JmjC domain of Gis1 is dispensable for transcriptional activation. FEMS Yeast Res. 2010; 10:793–801. [PubMed: 20868382]
42. Swinnen E, Wanke V, Roosen J, Smets B, Dubouloz F, Pedruzzi I, Cameroni E, De Virgilio C, Winderickx J. Rim15 and the crossroads of nutrient signalling pathways in Saccharomyces cerevisiae. Cell Div. 2006; 1:3. [PubMed: 16759348]
43. Geng J, Nair U, Yasumura-Yorimitsu K, Klionsky DJ. Post-Golgi Sec proteins are required for autophagy in Saccharomyces cerevisiae. Mol Biol Cell. 2010; 21:2257–2269. [PubMed: 20444978]
44. Longtine MS, McKenzie A III, Demarini DJ, Shah NG, Wach A, Brachat A, Philippsen P, Pringle JR. Additional modules for versatile and economical PCR-based gene deletion and modification in *Saccharomyces cerevisiae*. Yeast. 1998; 14:953–961. [PubMed: 9717241]

45. Govin J, Dorsey J, Gaucher J, Rousseaux S, Khochbin S, Berger SL. Systematic screen reveals new functional dynamics of histones H3 and H4 during gametogenesis. Genes Dev. 2010; 24:1772–1786. [PubMed: 20713519]

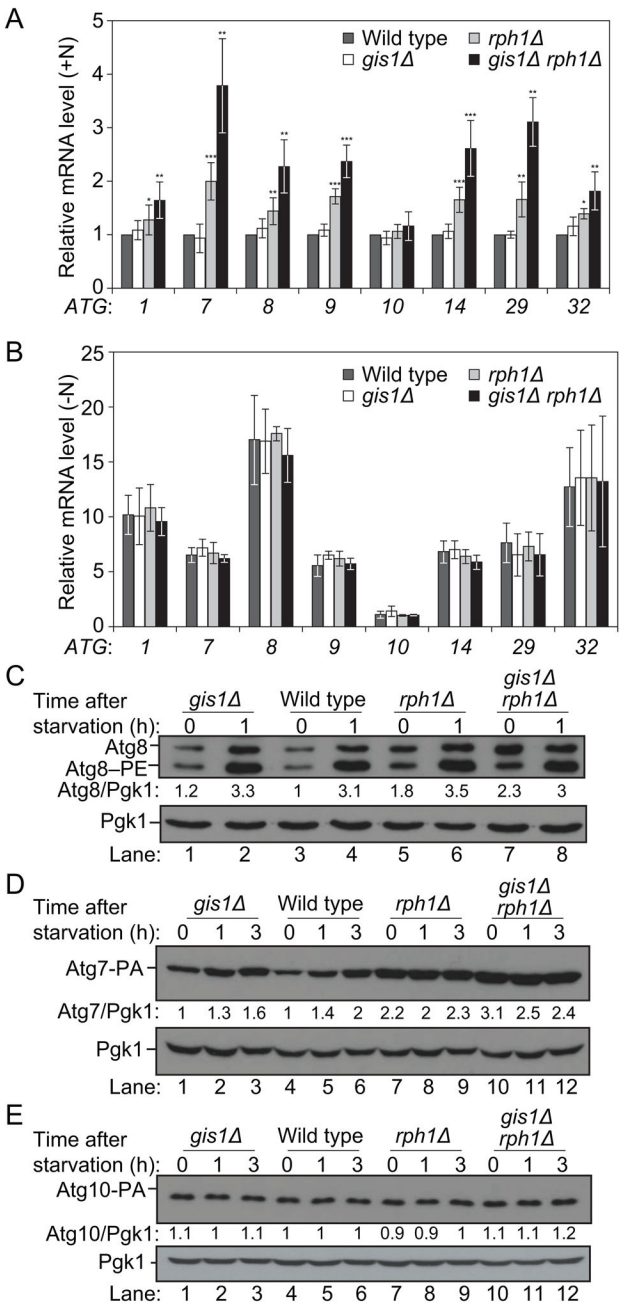

Figure 1. Rph1 represses the expression of nitrogen-sensitive *ATG* genes in nutrient-replete conditions

(A–B) Rph1 represses the expression of *ATG1*, *ATG7*, *ATG8*, *ATG9*, *ATG14* and *ATG29* in nutrient-replete conditions. Wild-type (YTS158), *rph1*Δ (YAB300), *gis1*Δ (YAB301) and *gis1*Δ *rph1*Δ (YAB302) cells were grown in YPD (+N) until mid-log phase (A) and then starved for nitrogen (−N) for 1 h (B). mRNA levels were quantified by RT-qPCR. Error bars indicate the standard deviation of the average of at least 3 independent experiments.

(C–E) Rph1 represses the expression of the Atg7 and Atg8 proteins. (C) For the analysis of Atg8, wild-type (YTS158, BY4742), *rph1*Δ (YAB300), *gis1*Δ (YAB301) and *gis1*Δ *rph1*Δ

(YAB302) cells were grown in YPD until mid-log phase and then starved for nitrogen for the indicated times. Protein extracts were analyzed by western blot with anti-Atg8 and anti-Pgk1 (loading control) antisera.

(D) To analyze Atg7 abundance, a protein A tag was integrated at the chromosomal locus. Wild-type (YAB312, BY4742), *rph1*Δ (YAB313), *gis1*Δ (YAB314) and *gis1*Δ *rph1*Δ (YAB315) cells were grown in the same conditions as in (C). Protein extracts were analyzed as in (C) with an antibody that detects PA or anti-Pgk1 antiserum.

(E) To analyze Atg10 abundance, a protein A tag was integrated at the chromosomal locus. Wild-type (YAB350, BY4742), *rph1*Δ (YAB351), *gis1*Δ (YAB352) and *gis1*Δ *rph1*Δ (YAB353) cells were grown in the same conditions as in (C). Protein extracts were analyzed as in (D).

(See also Figure S1, Table S1 and Table S2.)

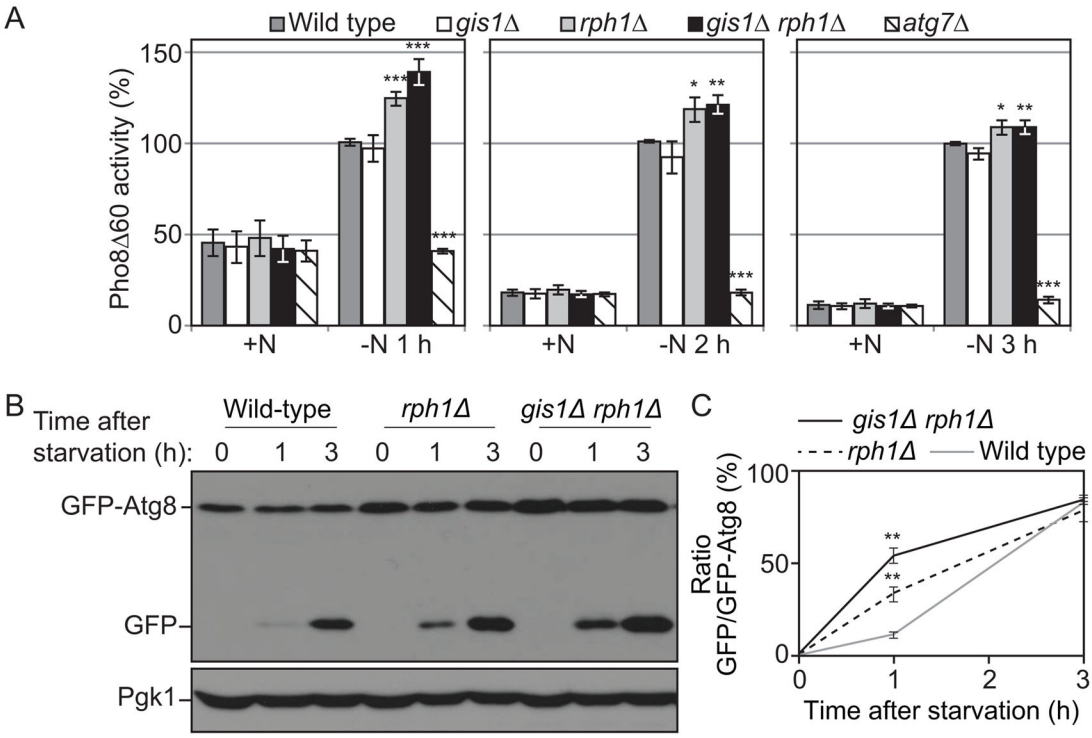

Figure 2. Rph1 negatively regulates autophagy

(A) Autophagy as measured by the Pho8Δ60 assay is increased in *rph1*Δ and *gis1*Δ *rph1*Δ cells. Wild-type (YTS158, BY4742), *rph1*Δ (YAB300), *gis1*Δ (YAB301), *gis1*Δ *rph1*Δ (YAB302) and *atg7*Δ (YAB292) cells were grown in YPD (+N) and then starved for nitrogen (−N) for the indicated times. The Pho8Δ60 activity was measured and normalized to the activity of wild-type cells after starvation, which was set to 100% at each time point. The data represent the average of 3 independent experiments; error bars indicate standard deviation.

(B) Autophagy as measured by the GFP-Atg8 processing is increased in *rph1*Δ and *gis1*Δ *rph1*Δ cells. Wild-type (YTS158, BY4742), *rph1*Δ (YAB300) and *gis1*Δ *rph1*Δ (YAB302) cells transformed with a CEN plasmid carrying a GFP-Atg8 construct were grown in rich selective medium and then starved for 1 and 3 h. Cells were collected and protein extracts were analyzed by western blot with anti-YFP antibody and anti-Pgk1 (loading control) antiserum.

(C) Quantification of (B). The ratio free GFP:GFP-Atg8 was measured and normalized to that of wild-type cells after 3 h starvation, which was set to 100%. Average values ± standard deviations of 2 independent experiments are indicated.

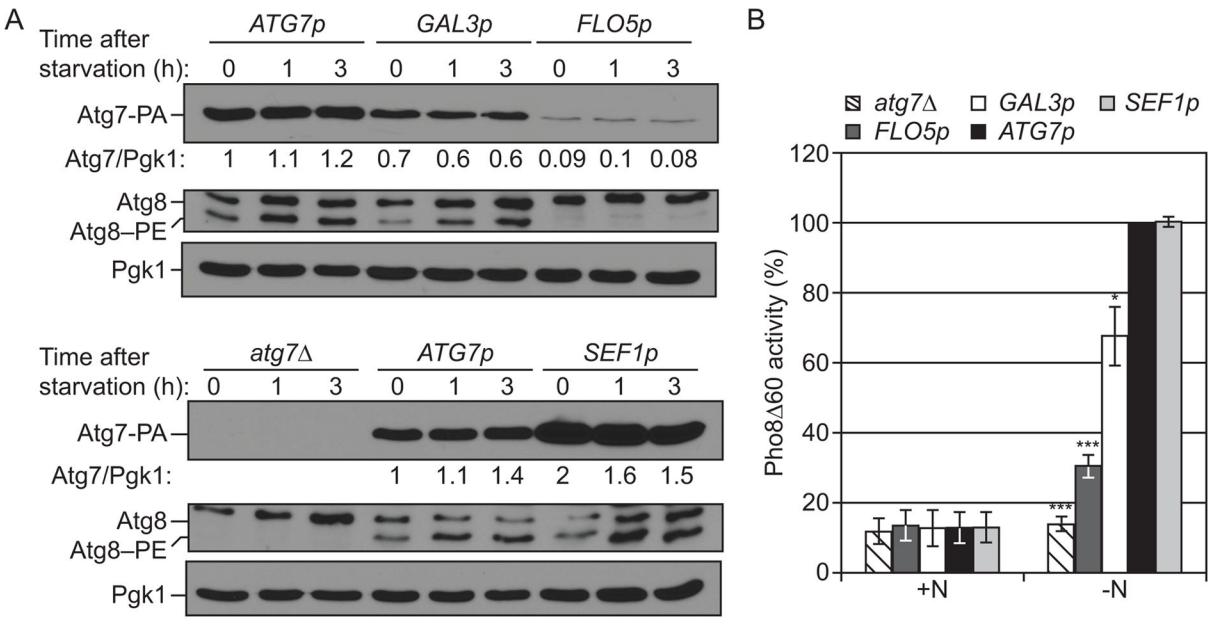

Figure 3. The level of Atg7 regulates autophagy

(A) Lowering the level of Atg7 results in a decrease in Atg8–PE conjugation and (B) a decrease in autophagy activity. *atg7*Δ cells (YAB292) were transformed with the *ATG7p-ATG7-PA*, *GAL3p-ATG7-PA*, *FLO5p-ATG7-PA*, or *SEF1p-ATG7-PA* plasmid or the corresponding empty plasmid (*pRS416-PA*). Cells were grown in rich selective medium (SMD-Ura) until mid log phase and then starved for nitrogen for the indicated times.

(A) Cells were collected and protein extracts were analyzed by western blot with either an antibody that recognizes PA, or anti-Atg8 and anti-Pgk1 (loading control) antisera.

(B) Cells were starved for 3 h. The Pho8Δ60 activity was measured and normalized to the activity of *ATG7p-ATG7-PA* cells, which was set to 100%. Data represent the average of 3 independent experiments.

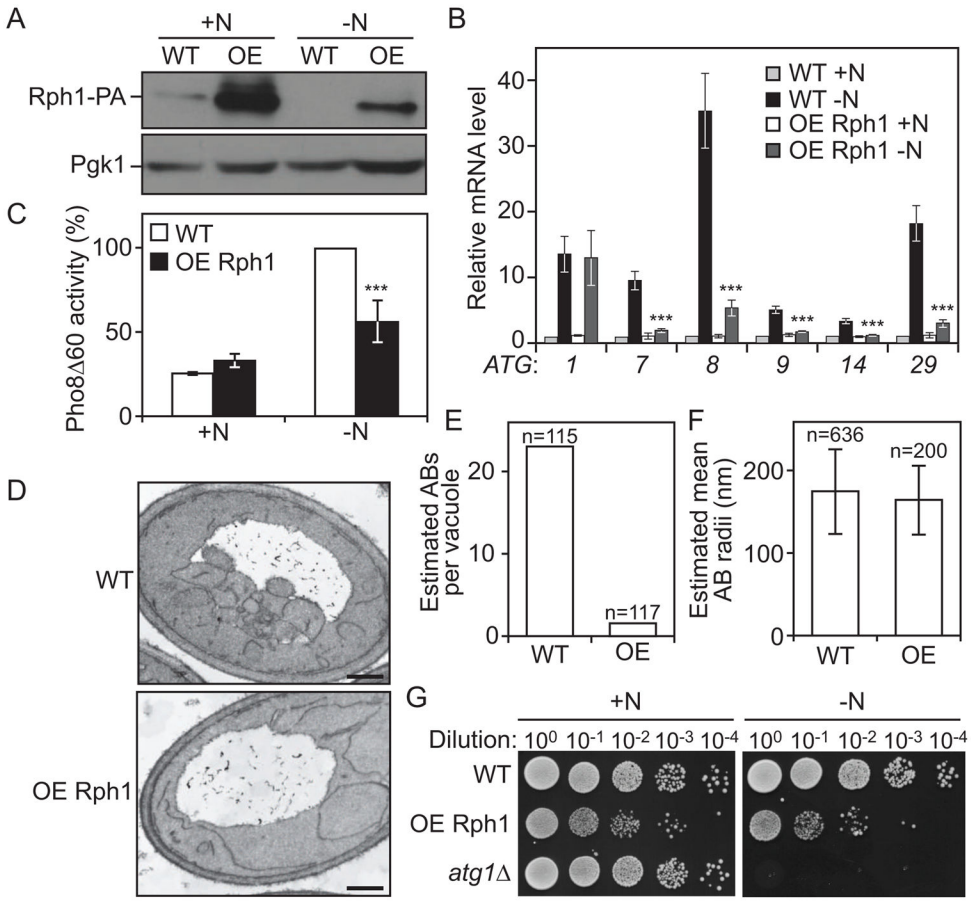

Figure 4. The overexpression of Rph1 inhibits autophagy and decreases cell survival in nitrogen starvation conditions

(A–C) Overexpressed Rph1 (*ZEO1p-RPH1-PA*) results in a block in *ATG* genes expression and autophagy flux. Rph1-PA cells (WT, YAB323, SEY6210) and cells overexpressing Rph1-PA (OE Rph1, YAB329) were grown in YPD (+N) until mid-log phase and then starved for nitrogen (−N).

(A) Cells were starved for 2 h, and protein extracts were analyzed by western blot with either an antibody that recognizes PA or anti-Pgk1 (loading control) antiserum.

(B) Total RNA of cells in mid-log phase (+N) as well as after 1 h of nitrogen starvation (−N) was extracted and the mRNA levels were quantified by RT-qPCR. The mRNA level of individual *ATG* genes was normalized to the mRNA level of the corresponding gene in Rph1-PA cells (WT), which was set to 1. Data represent the average of 3 independent experiments ± standard deviation.

(C) The Pho8Δ60 activity was measured and normalized to the activity of Rph1-PA cells (WT) after 2 h of nitrogen starvation (−N), which was set to 100%. Error bars indicate standard deviation of 3 independent experiments.

(D–E) Rph1 overexpression blocks the biogenesis of autophagic bodies. Wild-type cells (WT, FRY143) and cells overexpressing Rph1 (OE Rph1, YAB346) were imaged using transmission electron microscopy after 2 h of nitrogen starvation.

(D) Representative TEM images showing a reduced accumulation of autophagic bodies in the vacuole of cells overexpressing Rph1 compared to wild type. Scale bar, 500 nm.
(E) Estimated average number of autophagic bodies (AB) per vacuole. Estimation was based on the number of autophagic body cross-sections observed by TEM [50]. Over 100 unique cells per strain were captured and analyzed.
(F) The estimated mean radii (in nm) of the original autophagic bodies (AB) observed by TEM in wild-type and OE Rph1 cells was analyzed as in (E).
(G) Rph1 overexpression reduces cell survival after prolonged nitrogen starvation. Rph1-PA cells (WT, YAB323, SEY6210), cells overexpressing Rph1-PA (OE-Rph1, YAB329) and *atg1*Δ cells (WLY192) were grown in YPD (+N) until mid-log phase and then starved for nitrogen for 15 days (−N). Dilutions as indicated were grown on YPD plates for 2 days, then imaged.
(See also Figure S2 and Table S3.)

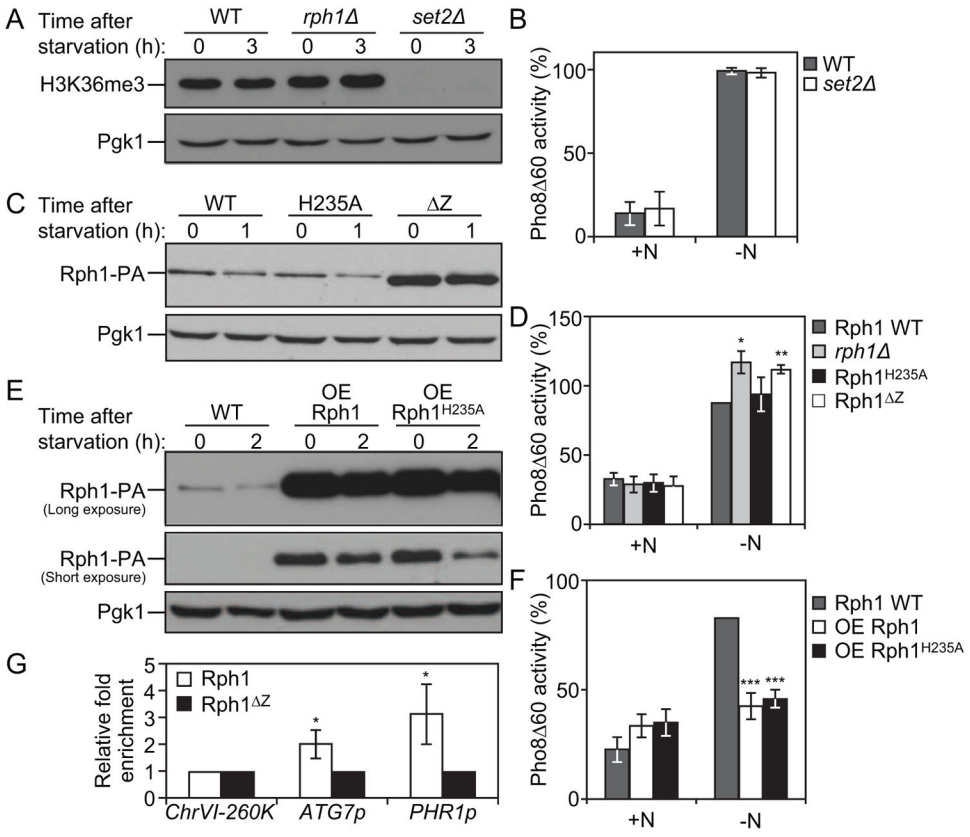

Figure 5. Rph1 DNA binding ability but not histone demethylase activity is required for its function in autophagy

(A) Wild-type (YTS158), *rph1*Δ (YAB300) and *set2*Δ (YAB318) cells were grown in YPD (+N) and then starved for nitrogen (−N) for 3 h. Protein extracts were analyzed by western blot with anti-H3K36me3 antibody and anti-Pgk1 (loading control) antiserum.

(B) Wild-type (YTS158, BY4742) and *set2*Δ (YAB318) cells were grown in YPD (+N) and then starved for nitrogen (−N) for 3 h. The Pho8Δ60 activity was measured and normalized to the activity of wild-type cells, which was set to 100%. For panels B, D, F and G, the data represent the average of 3 independent experiments ± standard deviation.

(C–D) *rph1*Δ cells were transformed with the *RPH1p-RPH1-PA* (Rph1, Wild-type), *RPH1p-RPH1^{H235A}-PA* (H235A), or *RPH1p-RPH1$^{\Delta Z}$-PA* (ΔZ) plasmids or the corresponding empty plasmid (*pRS461-PA, rph1*Δ). Cells were grown in rich selective medium (SMD-Ura) until mid-log phase and then starved for nitrogen for 1 h.

(C) The stability of Rph1 mutants was analyzed by western blot with either an antibody that recognizes PA or anti-Pgk1 (loading control) antiserum.

(D) The Pho8Δ60 activity was measured and normalized to the activity of wild-type Rph1 cells after 1 h of nitrogen starvation (−N), which was set to 100%.

(E–F) Rph1-PA cells (WT, YAB366) and cells overexpressing Rph1-PA (OE Rph1, YAB363) or Rph1^{H235A}-PA (OE Rph1^{H235A}, YAB364) were grown in YPD (+N) until mid-log phase and then starved for nitrogen for 2 h (−N).

(E) Protein extracts were analyzed by western blot with either an antibody that recognizes PA or anti-Pgk1 (loading control) antiserum.

(F) The Pho8Δ60 activity was measured and normalized to the activity of wild-type cells after 2 h of nitrogen starvation (−N), which was set to 100%.
(G) Rph1-PA binds the *ATG7* promoter. *rph1*Δ cells transformed with the *RPH1p-RPH1-PA* (Rph1) or *RPH1p-RPH1*$^{\Delta Z}$*-PA* (Rph1$^{\Delta Z}$) plasmids were analyzed by ChIP. ChIP was conducted on the *ATG7* promoter (*ATG7p*), a large non-coding region located at 260 kb on chromosome VI (*ChrVI-260K*) which was used as a negative control, and on the *PHR1* promoter (*PHR1p*) which was used as a positive control. Results were normalized to the input DNA and calibrated to the ChrVI-260K PCR product; results are presented as fold-enrichment of Rph1 binding compared to Rph1$^{\Delta Z}$, which was set to 1.
(See also Figure S3, Table S4 and Table S5.)

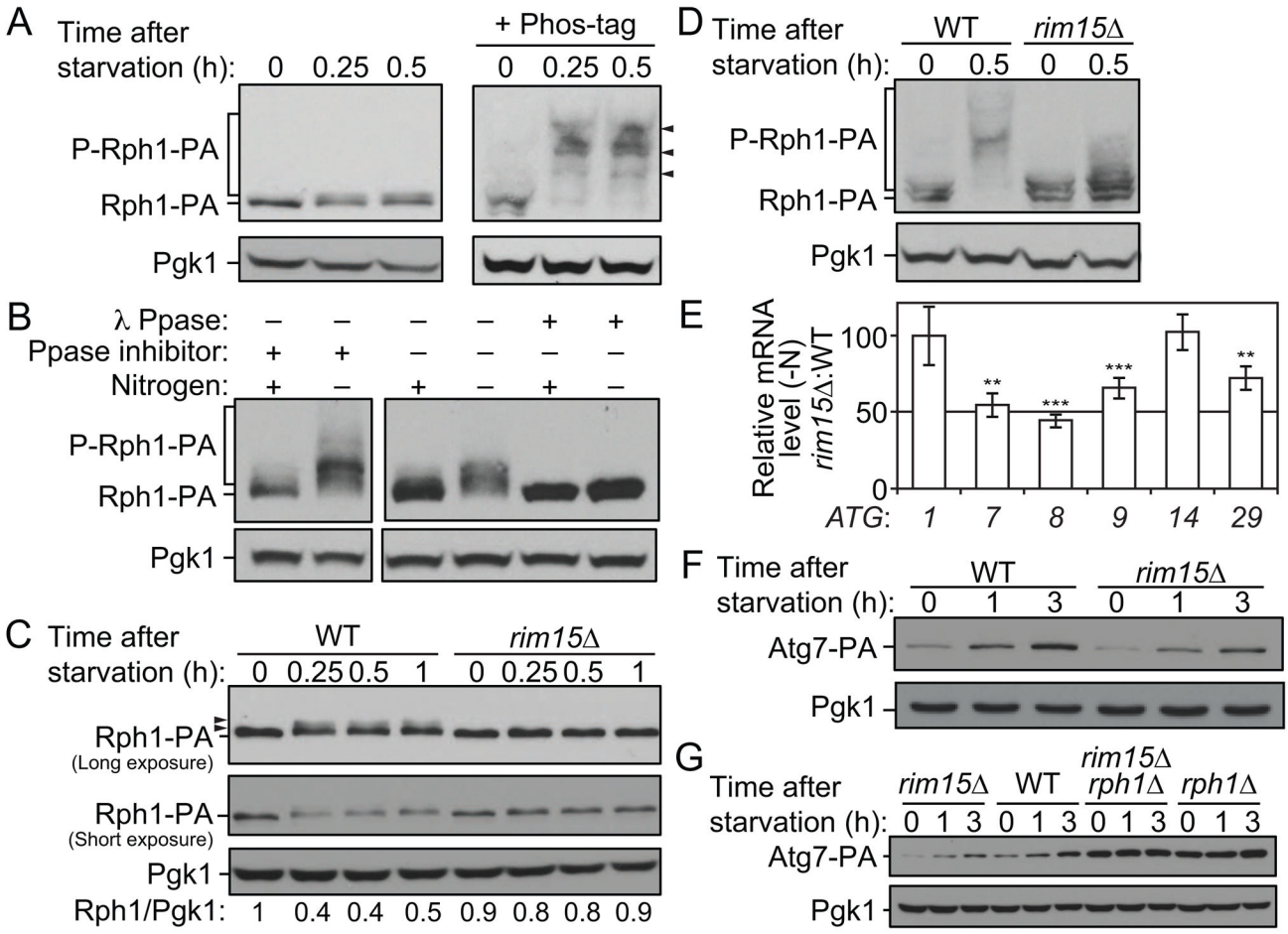

Figure 6. Rim15-dependent phosphorylation of Rph1 upon nitrogen starvation releases its repression on *ATG* gene expression and autophagy

(A–B) Rph1 is phosphorylated upon nitrogen starvation. Rph1 was chromosomally tagged with PA tag and Rph1-PA cells (YAB308) were grown in YPD until mid-log phase and then starved for nitrogen for the indicated times.

(A) Protein extracts were analyzed by western blot with or without 50 μM Phos-tag as indicated and with either an antibody that recognizes PA or anti-Pgk1 (loading control) antiserum. Arrowheads indicate shifts in molecular weight of Rph1-PA suggesting phosphorylation.

(B) Rph1-PA band shifts represent phospho-isoforms of the protein. Cells were lysed with or without phosphatase (Ppase) inhibitors. An aliquot of cell lysates was incubated at 30°C for 90 mintes in λ-phosphatase buffer with or without λ-phosphatase (λ Ppase). The reaction was stopped and proteins were precipitated by addition of 10% trichloroacetic acid. Protein extracts were analyzed by western blot as in (A) from gels containing Phos-tag.

(C–D) Rph1 phosphorylation upon nitrogen starvation is blocked in *rim15*Δ cells. *RPH1* was chromosomally tagged with PA in wild-type (WT) and *rim15*Δ cells. Cells were grown in YPD until mid-log phase and then starved for nitrogen for the indicated times. WT (YAB308) and *rim15*Δ cells (YAB341) were collected and protein extracts were analyzed

by western blot with either an antibody that recognizes PA or anti-Pgk1 (loading control) antiserum. (D) Protein extracts were analyzed by western blot as in (B).
(E) The deletion of *RIM15* reduces the induction of *ATG* gene expression after nitrogen starvation. WT (YAB308) and *rim15*Δ (YAB341) cells were grown in YPD until mid-log phase and then starved for 1 h (−N). mRNA levels were quantified by RT-qPCR. The mRNA levels of individual *ATG* genes were normalized to the mRNA level of the corresponding gene in WT cells in nitrogen starvation condition (−N), which was set to 100. Data represent the average of at least 3 independent experiments ± standard deviation.
(F) *ATG7* was chromosomally tagged with PA in WT (YAB312) and *rim15*Δ (YAB342) cells. Cells were grown in YPD until mid-log phase and then starved for nitrogen for the indicated times. Protein extracts were analyzed by western blot with either an antibody that recognizes PA or anti-Pgk1 (loading control) antiserum.
(G) *ATG7* was chromosomally tagged with PA in WT (YAB312), *rim15*Δ (YAB342), *rph1*Δ (YAB313) and *rim15*Δ *rph1*Δ (YAB347) cells. Proteins extracts were analyzed as in (F). (See also Figure S4.)

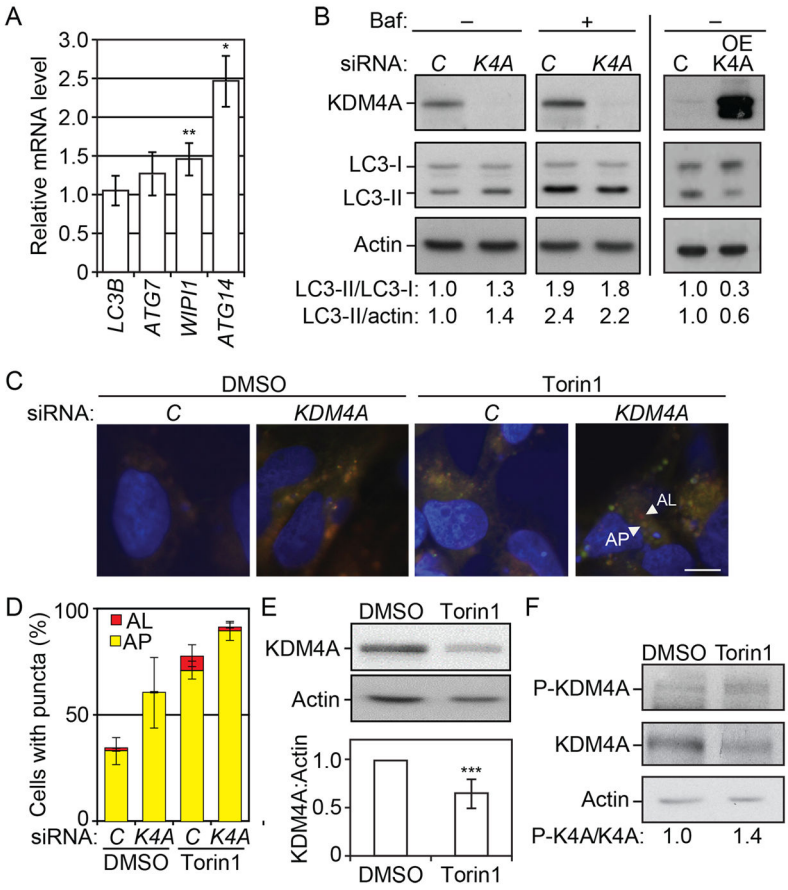

Figure 7. *KDM4* regulates autophagy in mammalian cells

(A) Transfected cells were grown for 48 h post transfection. Total RNA was extracted and the mRNA levels were quantified by RT-qPCR. The mRNA level of individual *ATG* genes was normalized to the mRNA level of the corresponding gene in the control cells (transfected with non-targeting siRNAs), which was set to 1. Error bars indicate the standard deviation of at least 3 independent experiments.

(B) Left panel: HeLa cells transfected with siRNA against *KDM4A* (*K4A*) show a reduction in the expression of KDM4A and a concomitant increase in the LC3-II/LC3-I and LC3-II/actin ratio compared to the cells transfected with non-targeting siRNAs (control, *C*). In the presence of bafilomycin A_1 (Baf), control and si*KDM4A* cells show a similar accumulation of LC3-II. Right panel: HeLa cells transfected with a plasmid overexpressing KDM4A (OE-KDM4A) show a decrease in the LC3-II/LC3-I and LC3-II/actin ratio compared to control cells (C). Total cell lysates were harvested 48 h after transfection and protein extracts were analyzed by western blot using antibodies to the indicated proteins.

(C–D) Cells were transfected with the mRFP-GFP-LC3 plasmid. On the subsequent day, cells were transfected with si*KDM4A* (*KDM4*) or non-targeting siRNAs (control, *C*). Cells were treated for 24 h with DMSO or 250 nM Torin1 as indicated.

(C) Cells were analyzed by fluorescence microscopy. Scale bar, 5 μm.

(D) Autophagy was determined by quantification of the number of cells with LC3-positive organelles. The histogram represents the mean of 3 independent experiments with SEM. AL, autolysosomes; AP, autophagosomes; *K4A*, *KDM4A*.

(E) KDM4A is degraded upon autophagy induction by Torin1. Cells were treated with 250 nM Torin1 for 24 h. Protein extracts were analyzed by western blot using antibodies to the indicated proteins. The average and standard deviation of 7 independent experiments are provided.

(F) Phosphorylation of KDM4A at Tyr547 is upregulated by treatment with Torin1. Cells were treated with Torin1 and protein extracts analyzed by western blot as in (E). K4A, KDM4A; P-KDM4A/P-K4A, phosphorylated KDM4A.